Progress In Electromagnetics Research B, Vol. 90, 21–41, 2021

Wearable Button-Like Dual-Band Central Antenna for Wireless Body Area Networks

Asmaa E. Farahat* **and Khlaid F. A. Hussein**

Abstract—A novel dual-band conical-helix/monopole antenna is proposed to operate as an on-body central antenna for Wireless Body Area Network (WBAN). The proposed antenna communicates in three ways: (i) off-body communication through its end-fire radiation with the ceil-mounted WiMax antenna at 5.8 GHz, (ii) on-body communication through its broadside radiation with the on-skin biosensor antennas at 3.0 GHz, and (iii) in-body communication with the in-body (implanted) biosensor antennas at 3.0 GHz. The characteristics of the proposed antenna are investigated through electromagnetic simulation and experimental measurements where a prototype of this antenna is fabricated for this purpose. The antenna is matched with 50 Ω coaxial feeder over the dual frequency bands, mounted on a copper circular disc, and covered with a very thin dielectric radom for mechanical protection. Such an antenna covered by the radom is shaped like a hemispherical button that can be attached to patient clothes and, hence, it can be considered as a wearable antenna. The radiation patterns obtained by experimental measurements show good agreement with those obtained by the CST® simulator and are shown to be appropriate for communication with the ceil-mounted WiMAX antenna and the biosensor antennas at 5.8 GHz and 3.0 GHz, respectively. The distribution of the microwave power density near the body surface is evaluated by simulation and experimental measurements to ensure the realization of the electromagnetic exposure safety limits. The Specific Absorption Rate (SAR) distribution inside the human tissues of concern is evaluated showing a safe level of electromagnetic exposure. Quantitative assessment of the WBAN communication system performance is achieved when the proposed antenna is employed as an on-body central antenna for the WBAN. Thanks to the optimized design of the proposed antenna the Bit-Error-Rate (BER) is shown to be very low even when the input power fed to the antenna is only 1 mW.

1. INTRODUCTION

Biosensors are mainly designed for the purpose of diagnostic, therapeutic and assistive applications in health-care, active living, and sports technology [1–3]. In Wireless Body Area Network (WBAN), to monitor a patient's health status, the implanted device collects various physiological data and wirelessly transmits the information to external medical devices in real time. The antenna design for this purpose faces great difficulties as the wireless communication medium is not through-the-air but uses the human tissues as part of the transmission channel. Human body is lossy in nature and also has high permittivity. Therefore, when designing an antenna for body sensor networks with proximity to the human body, the performance will change in a noticeable way. It is hard to apply the traditional theory of the antenna and channel to observe their normal characteristics separately. The antenna when being mounted on a lossy, dispersive medium (e.g., human body) acts as a radiator that is affected by this propagation medium. Therefore, the concept of the antenna de-embedding is the solution for dealing with the antenna on its own, modeling it, and taking into consideration the effect of the surrounding medium [4, 5].

Received 20 October 2020, Accepted 10 November 2020, Scheduled 16 December 2020
* Corresponding author: Asmaa Elsayed Farahat (asmaa@eri.sci.eg).
The authors are with the Microwave Engineering Department, Electronics Research Institute, Cairo 11843, Egypt.

The factors affecting the antenna design include antenna impedance matching, radiation pattern, Specific Absorption Rate (SAR), size compactness, space constraints, desired radiation characteristics, light weight, multi-band operation, interference mitigation, positioning, and stable performance with the variation of the gap between the antenna and the human body. To comply with safety guidelines, a limitation is applied to the effective power radiated from the antenna. This power limitation adds extra challenge to the antenna design in the human body lossy medium [6, 7].

For wearable antennas intended for on/off-body wireless communications, the challenge is to design an antenna with dual operation modes, and each mode has its specific radiation characteristics. For the first mode, the antenna is used for on-body communications to collect vital information from the human body (i.e., from the in-body and on-body biosensors). This requires the antenna to have wide-beam or omnidirectional radiations in the plane parallel to the human body surface to provide maximum coverage over the body. This can be achieved by minimizing the radiations that are away from the human body (i.e., off-body). By introducing a null in the direction normal to the body, we can suppress off-body radiations and can enhance on-body radiations. In the second mode of operation, the antenna is used to transmit the collected information towards the outside WiMAX for example. In this case, the radiated beam can be directed towards the receiving device placed away from the patient's body [6, 7].

The objective of this paper is to provide an optimized design of a novel conical-helix/monopole antenna proposed to operate as a central on-body antenna in WBANs. The far-field radiation patterns are evaluated at the two operational frequency bands (3.0 and 5.8 GHz). The near-field distribution at the possible locations of the on-skin and implantable (in-body) biosensor antennas is evaluated at 3.0 GHz.

The antenna losses are usually dominated by its Ohmic losses which are caused by conductor and dielectric losses. When the conducting parts of an antenna are made of a metal of very high conductivity such as copper or gold, the antenna Ohmic losses are dominated by the dielectric loss. For example, the Ohmic losses of a microstrip patch antenna are dominated by the dielectric substrate loss. The conical-helix/monopole antenna proposed in the present work is made of conducting (copper) parts, and hence, its Ohmic losses can be negligible. For this reason and thanks to the perfect impedance matching and the proper radiation patterns for on/off-body communications, the conical-helix/monopole antenna proposed in the present work requires very low input power to achieve all the required characteristics addressed above and to enable high performance of the WBAN communication system at the two operational frequency bands. The proposed antenna has the advantage of being made of only conducting wires and thereby reducing the dielectric loss encountered in the other antennas containing dielectric parts such as the microstrip patch antennas.

The assessment of the WBAN communication system regarding the Signal-to-Noise-Ratio (SNR) and the corresponding Bit-Error-Rate (BER) is performed assuming that the modulation system used for communication between the central on-body antenna and the biosensor antennas is M-ary PSK. It is required that the radiation performance of the proposed antenna enables the achievement of the required BER using low level of its input power so as to get the lifetime of the biosensor batteries as long as possible and to get the SAR in the human tissues as low as possible.

2. THE PROPOSED DUAL-BAND CONICAL HELIX/MONOPOLE ANTENNA

This section is concerned with the description of the conical-helix/monopole antenna proposed to work as on-body central antenna in WBANs. This antenna is dual-band and designed to communicate (through its far-field pattern) with the ceil-mounted WiMAX antenna at 5.8 GHz and to communicate (through either its near-field or far-field pattern) with the on-skin and in-body (implanted) biosensor antennas at 3.0 GHz. The monopole is a part of the wire antenna structure that is responsible for broadside radiation at 3.0 GHz whilst the conical-helix produces end-fire radiation pattern at 5.8 GHz. The proposed antenna has a small size as shown in Figure 1(a) and can be mounted on the human body as a button attached to the clothes as shown in Figure 1(b). Excluding the SMA connector, the antenna diameter is 20 mm, and the antenna height is 18.5 mm.

The proposed antenna is designed to have a balloon-shaped radiation pattern to communicate with the WiMAX system at 5.8 GHz and to have a broad-side radiation pattern to communicate with the on-body and in-body biosensor antennas at 3.0 GHz. The configuration of the antenna system required for

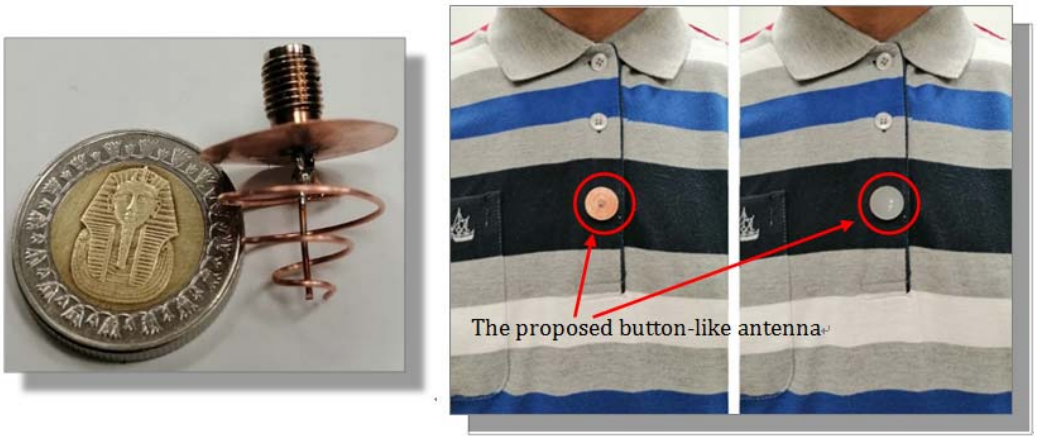

Figure 1. The fabricated prototype of the proposed conical-helix/monopole antenna, (a) the antenna size compared with the size of a standard one-inch coin, (b) the uncovered antenna attached to the clothes as a button, (c) the antenna covered with the radom and attached to the clothes as a button.

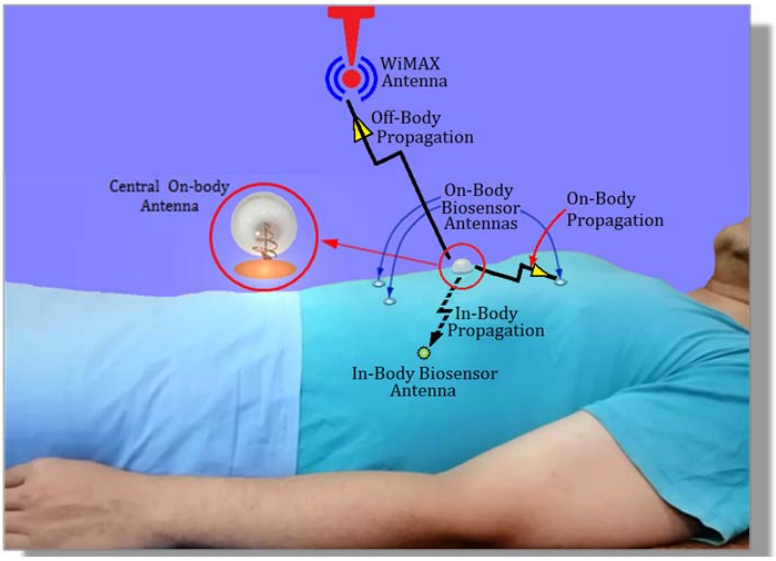

Figure 2. The conical-helix/monopole antenna proposed in the present work is attached to clothes of the patient as wearable button antenna. The on-body central antenna communicates with the on-body and in-body biosensor antennas via on-body/in-body microwave propagation. The on-body antenna connects the WBAN to the WiMAX through off-body (far-field) radiation into free space.

on/off-body communications in the WBANs is illustrated in Figure 2, where the conical-helix/monopole antenna proposed in the present work to play the role of a central on-body antenna can be attached to clothes of the patient as a wearable button-like antenna.

The geometric model of the dual-structures of the proposed on-body antenna is shown in Figure 3. The monopole length is H_M; the height, base diameter, and apex half-angle of the conical helix are H_H, D_H, and θ_H, respectively.

The design of the proposed antenna permits the use of low power (a few milli-Watts) for communication with the on-body and in-body biosensor antennas at 3.0 GHz and allows the use of higher level of power while communicating with the WiMAX antenna (at 5.8 GHz). The power consumption is,

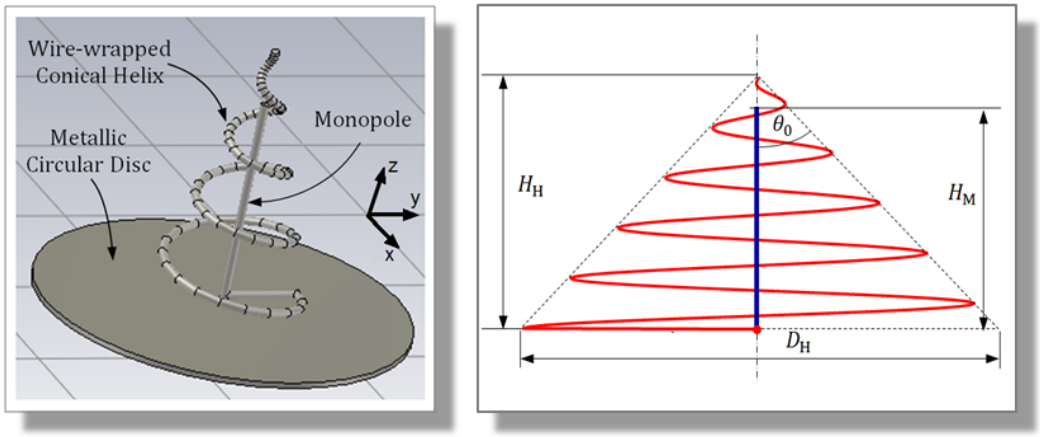

Figure 3. Geometry of the conical-helix/monopole antenna, (a) geometric model of the proposed antenna in the CST® simulator, (b) schematic antenna dimensional parameters.

thus, optimized leading to low level of the SAR in the human tissues and long life-time of the batteries required to energize the transceiver attached to the central on-body antenna and the biosensor antennas.

3. ANTENNA AND BODY MODEL FOR ELECTROMAGNETIC SIMULATION

For realistic electromagnetic simulation, the human body below the antenna can be replaced by the three-layer (skin-fat-muscle) model [2] shown in Figure 4. The electric properties of the three tissue types at 3.0 GHz and 5.8 GHz are listed Table 1.

The geometric model of the proposed conical-helix/monopole mounted directly on the top antenna in the commercially available CST® simulator is presented in Figure 5. The monopole has a length

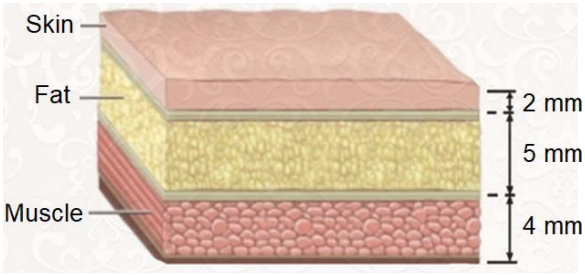

Figure 4. Three-layer (skin-fat-muscle) model of the human body for the simulation scenareo of electromagnetic radiation from on-body antenna radiation.

Table 1. Electric properties of the concerned types of the human tissues at 3.0 GHz and 5.8 GHz (deduced from [2]).

Tissue Type	Mass Density, ρ (kg/m^3)	Dielectric Constant, ε_r		Conductivity, σ (S/m)	
		$f = 3.0$ GHz	$f = 5.8$ GHz	$f = 3.0$ GHz	$f = 5.8$ GHz
Skin	1109	37	35.11	1.95	3.72
Fat	911	5.1	4.95	0.16	0.29
Muscle	1090	51.2	48.48	2.90	4.96

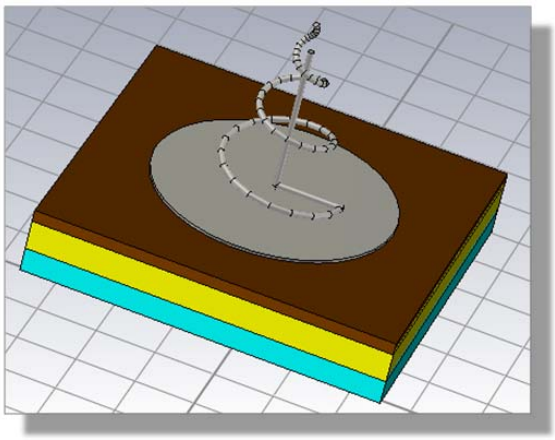

Figure 5. Model of the proposed conical-helix/monopole on-body antenna placed on the three-layer (skin-fat-muscle) model of the human body(the model used in the simulator is much larger than that indicated in the figure); the antenna has the dimensional parameters $N_T = 3$, $H_H = 18.5\,\text{mm}$, and $D_H = 20\,\text{mm}$, $H_M = 18.5\,\text{mm}$.

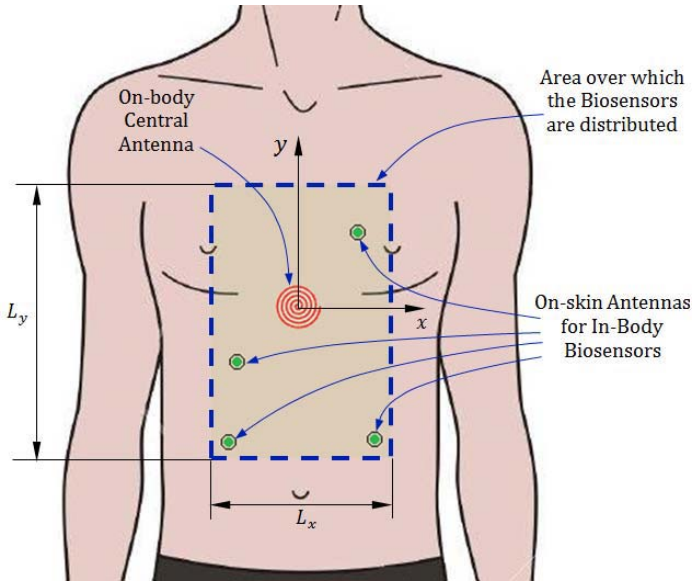

Figure 6. The radiation from the on body antenna covers the chest/belly area surrounded by the blue dashed rectangle and occupied by the biosensor antennas.

of $H_M = 18.5\,\text{mm}$, and the height, base diameter, and apex half-angle of the 3-turn conical helix are, respectively, $H_H = 20\,\text{mm}$, $D_H = 20\,\text{mm}$, and $\theta_H = 26.5°$. The diameters of the circular copper plates used for simulation range from 20 mm to 40 mm. The CST® simulator is used to evaluate the far-field pattern at 5.8 GHz. The three-layer planar structure described in Figure 4 is placed just below the antenna base as shown in Figure 5 to represent the human body.

The evaluation of the field distribution on the top surface of the skin layer is a necessary requirement for the performance assessment of the on-body communications between the proposed central antenna and distributed on-skin biosensor antennas. Also, the calculation of the electric field penetrating the human tissues namely the skin, fat, and muscle tissues is necessary for the evaluation of the SAR in these tissues and for the evaluation of the power received by the in-body biosensor antennas.

It should be noted that the human body region of concern in the present study is the area surrounded

by the blue dashed rectangle shown in Figure 6. The field distribution over this area is evaluated under the assumption of a flat surface of this region of the body. It should be noted that this rectangular area has the dimensions $L_x = 20\,\text{cm}$ and $L_y = 30\,\text{cm}$; these dimensions are considered throughout the following presentations and discussions of numerical results unless otherwise indicated.

4. FABRICATION OF THE CONICAL-HELIX/MONOPOLE ANTENNA PROTOTYPE

This section is concerned with the procedure of fabricating a prototype for the proposed conical-helix/monopole antenna. The antenna is fabricated using a copper wire of 0.5 mm. Two circular copper discs of 40 mm and 20 mm diameters are used for experimental assessment. Due to high conductivity of the copper and the absence of any dielectric parts, the Ohmic losses of this antenna are negligible.

4.1. Constructing the Conical-Helix and Monopole Wires

For the fabrication of a prototype of the proposed antenna, a copper wire is wrapped to take the shape of the conical helix with the dimensions given in Section 3. A wire wrapped in the right-hand sense produces right-hand circularly polarized field whereas a wire wrapped in the left-hand sense, as that shown in Figure 7(a), produces left-hand circularly polarized field.

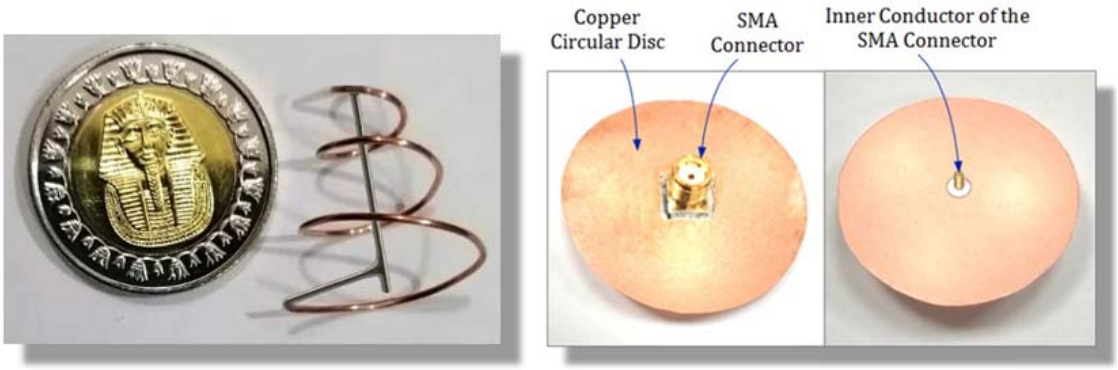

Figure 7. A copperwire is wrapped to form a conical helix and then welded to a straight wire to form the dual wire structure of the conical-helix/monopole antenna proposed to play the role of a central on-body antenna for WBAN, (a) the dual wire structure of the antenna, (b) the circular copper disc on which the wire structure is mounted.

The wrapped conical-helix is then welded at its base to a straight wire (quarter-wavelength monopole at 3.0 GHz) to form a complete wire structure of the antenna as shown in Figure 7(a). A ground plane and a feeding coaxial connector are necessary for the operation of such a conical-helix antenna/monopole. A circular copper disc of 4 cm diameter is prepared for this purpose, and an SMA coaxial connector is mounted with its outer conductor welded to the circular disc as shown in Figure 7(b). The dual-structures of the wire antenna, shown in Figure 7(a), are mounted on a circular copper plate by welding the monopole extension at the cone base to the inner conductor of the SMA connector to form the entire antenna structure shown in Figure 8(a). A foam tube can be used to enclose the wire monopole for electric insulation between the monopole and the conical helix.

4.2. Adding Impedance Matching Elements to the Antenna Structure

To minimize the return loss, the wire antenna should be matched to a 50 Ω SMA coaxial connector. The conical-helix antennas are characterized by an advantage of low imaginary part of the input impedance at the design frequency for end-fire radiations. Unfortunately, they are also characterized by a resistive

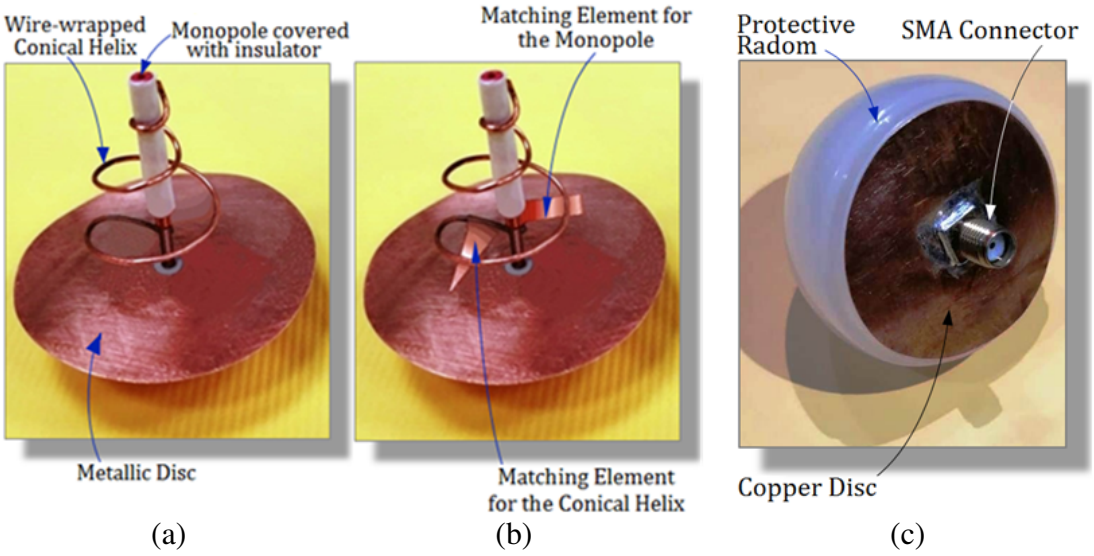

Figure 8. The conical-helix/monopole structure is mounted on a circular copper disc and connected to the inner conductor of an SMA connector (a) without impedance matching, (b) with a triangular patch connected to the conical helix and another rectangular patch connected to the monopole near the feed point for impedance matching at 5.8 and 3.0 GHz, (c) the matched antenna covered with hemispherical radom for mechanical protection.

part of the impedance that is much smaller than 50 Ω. The real part of the impedance can be increased to 50 Ω by attaching a small conductive triangular patch to the wire of the antenna near the feed point as shown in Figure 8(b). On the other hand, the quarter-wavelength straight wire monopole antennas are characterized, at resonance, by very low imaginary part of the input impedance and a resistive part that is greater than 50 Ω. The real part of the monopole impedance can be decreased to 50 Ω by attaching a small conductive rectangular patch near the feed point as shown in Figure 8(b). The size and location of such triangular and rectangular patches used for impedance matching can be experimentally adjusted while being attached to the antenna structure with the aid of a Vector Network Analyzer (VNA) so as to minimize the reflection coefficient $|S_{11}|$ over the frequency bands of interest.

4.3. Covering the Wire Antenna with Hemispherical Radom for Mechanical Protection

For protecting the wrapped wires of the fabricated helical antennas from deformation due to unavoidable mechanical stresses, a hemispherical radom of very thin dielectric material is used to cover the antenna structure as shown in Figure 8(c). As this radom is made of very thin dielectric material ($\varepsilon_r = 1.5$), which is almost electromagnetically transparent at the microwave frequencies and, consequently, has no effect on the antenna characteristics. Finally, for the purpose of microwave measurement, the antenna is connected to a flexible 50 Ω coaxial cable through the SMA connector mounted on the circular disc.

5. ASSESSMENT OF THE WBAN COMMUNICATION SYSTEM PERFORMANCE

For transmitting information through physical channels in the communication systems, the design of these systems requires to construct mathematical models which show the most important features of the transmission media. This section is concerned with the quantitative description of shared wireless transmission model of the WBAN. The purpose of building such a channel model is the assessment of the communication system performance regarding the SNR and the corresponding BER assuming that the modulation system is M-ary PSK.

5.1. Channel Modeling for WBAN Communications and Assessment of Noise Power

It is assumed that the unavoidable thermal noise and the ambient microwaves interfering with the signal carrying the information of concern can be modeled as Additive White Gaussian Noise (AWGN) with power spectral density $N_0/2$ (W/Hz). In such a model, the transmitted signal $s(t)$ is distorted by such type of noise $n(t)$, and consequently, the signal received at the isotropic biosensor antennas distributed over the human body, $x(t)$, can be expressed in the time-domain as follows.

$$x\left(t\right) = s\left(t\right) + n(t) \tag{1}$$

The discrete time samples of the noise function can be expressed as follows.

$$n_p = n\left(t_p\right), \quad t_p = \left(p-1\right)\Delta t, \ p = 1, 2, .., P \tag{2}$$

where P is the total number of time samples that cover the time period required for simulation of the transmission/reception process of large enough number of symbols.

For such a simulation, the values of n_p, for $p = 1, 2, ..., P$, can be generated using a Gaussian probability distribution function of the following form.

$$g_n = \frac{1}{\sigma_n\sqrt{2\pi}} e^{-\frac{n^2}{2\sigma_n^2}} = \frac{1}{\sqrt{2\pi N_0}} e^{-\frac{n^2}{N_0}} \tag{3}$$

with $\sigma_n^2 = N_0/2$.

In the frequency-domain, the received signal can be expressed, in a complex (phasor) diagram, as follows.

$$r_x e^{j\varphi_x} = r_s e^{j\varphi_s} + r_n e^{j\varphi_n} \tag{4}$$

where r_x, r_s, and r_n are the magnitudes of the received, transmitted, and noise signals, respectively, whereas φ_x, φ_s, and φ_n are the associated phases for these signals, respectively.

Assuming that the bandwidth dedicated for data transfer between the biosensor antennas and the central on-body antenna is $B_W = 2R_b$, where R_b is the bit rate, the noise power can be evaluated as:

$$P_N = \frac{1}{2} N_o B_W \tag{5}$$

where P_N is the noise power.

To model the AWGN numerically, the phase, φ_n, associated with the noise can be generated using a uniformly distributed probability distribution function over the interval $0 \leq \varphi_n \leq 2\pi$, whereas it may be convenient to set the magnitude of the noise, r_n, to a constant value as follows.

$$r_n = \sqrt{P_N} \tag{6}$$

Thus, the representation of the received signal in the complex plane (for a constellation diagram) due to the addition of the AWGN can be described as shown in Figure 9.

5.2. Assessment of Signal Strength and SNR over the Skin of the Human Body in Communication System of the WBAN

The angular distribution of the transmitted signal strength (power) due to the on-body central antenna can be evaluated as:

$$P_s\left(R, \theta, \phi\right) = P_{Rx}(R) S\left(\theta, \phi\right) \tag{7}$$

where $S(\theta, \phi)$ is the power radiation pattern of the central on-body antenna, and $P_{Rx}(R)$ is the level of the signal at a distance R from this antenna. If the propagation were only in free space, the received power would be expressed as follows.

$$P_{Rx}(R) = P_{Tx}\left(\frac{\lambda}{4\pi R}\right)^2 \tag{8}$$

For more accurate results, the received power level, $P_{Rx}(R)$, is assessed by electromagnetic simulation. The SNR for an on-body sensor antenna located at (R, θ, ϕ) can be calculated as follows.

$$\text{SNR} = \frac{P_s}{P_N} = \frac{P_{Rx}(R) S\left(\theta, \phi\right)}{\frac{1}{2} N_o B_W} \tag{9}$$

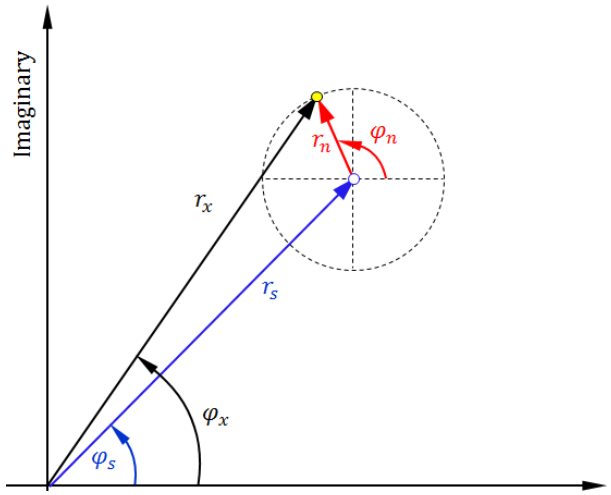

Figure 9. Representation of the received signal, $r_x e^{j\varphi_x}$, for a specific transmitted symbol, $r_s e^{j\varphi_s}$, after adding the AWGN $r_n e^{j\varphi_n}$.

5.3. Assessment of the BER through Numerical Simulation

The following expression gives the relation between the SNR and the ratio E_b/N_o.

$$\mathrm{SNR} = \frac{P_s}{P_N} = \frac{E_b R_b}{\frac{1}{2} N_o B_W} \tag{10}$$

In another form, the relation in Eq. (10) can be expressed as

$$(E_b/N_o)_{\mathrm{dB}} = \mathrm{SNR}_{\mathrm{dB}} - (R_b/B_W)_{\mathrm{dB}} - 3 \tag{11}$$

It should be noted that the quantity (R_b/B_W) is defined as the spectral efficiency of the communication system.

In the present work, the dependence of the BER on the SNR (or E_b/N_o) is assessed through numerical simulation by generating random symbols (uniformly distribution) associated with noise samples (Gaussian distribution). Also, the calculation of the BER depends on the modulation technique implemented in the communication system of the WBAN. The Mary-PSK is used for the performance assessment of a WBAN employing the central on-body conical-helix/Monopole antenna proposed in the present work.

6. RESULTS OF ELECTROMAGNETIC SIMULATION AND EXPERIMENTAL MEASUREMENTS

This section is concerned with the presentation and discussion of the electromagnetic simulation results and experimental measurements to study the characteristics of the conical-helix/monopole antenna proposed to work as on-body central antenna for WBAN. The presented results are also concerned with investigating the performance of the on/off-body communication system employing the proposed antenna including the power consumption, the SNR and BER, and the associated SAR in the different human tissues near the body surface (skin, fat and muscle).

6.1. Return Loss and Impedance Bandwidth of the Proposed On-Body Antenna

The reflection coefficient at the antenna port is measured using VNA of the Agilent FieldFox N9918A. The frequency response of the reflection coefficient $|S_{11}|$ is measured over a wide range of frequency. The experimental measurements are compared to the numerical results obtained by electromagnetic simulation using the commercially available CST® microwave studio suite.

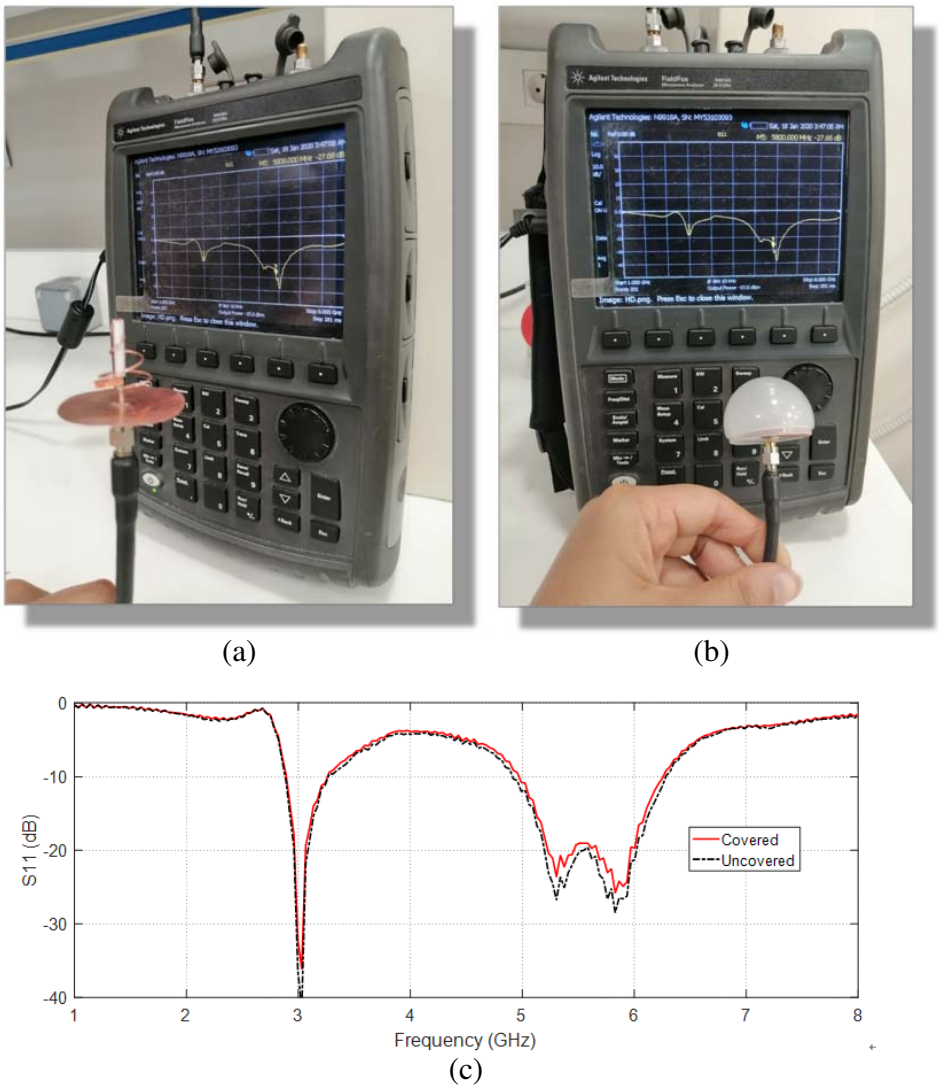

Figure 10. Measurement of the reflection coefficient $|S_{11}|$ of the conical-helix/monopole antenna using the VNA of the Agilent Field Fox N9918A, (a) uncovered antenna, (b) antenna covered with the hemispherical radom, (c) comparison between the frequency responses of $|S_{11}|$ in the two cases.

The experimental setup for measuring the frequency response of the reflection coefficient $|S_{11}|$ of the conical-helix/monopole antenna is shown in Figure 10. The comparison between measurement curves appearing on the screen of the measurement device and presented in Figure 10(c) shows that the reflection coefficient of the conical-helix/monopole antenna is almost unaffected by the placement of the radom to cover the antenna.

Figure 11 presents the measured frequency responses of the reflection coefficient $|S_{11}|$ of the conical-helix/monopole antenna. Both the experimental measurements and simulation results show that the antenna impedance is matched to $50\,\Omega$ over the two frequency bands of interest. The impedance matching bandwidth (for $|S_{11}| \leq -10\,\text{dB}$) according to the experimental measurement is about 11% at 3.0 GHz and about 22% at 5.8 GHz. The sharp minimum of the $|S_{11}|$ frequency response shows that the antenna is resonant at the frequency 3.0 GHz. This corresponds to the first resonance of the quarter-wavelength monopole. However, the bandwidth at 3.0 GHz is fairly acceptable for high-speed data transmission between the biosensor antennas and the proposed central on-body antenna. On the other hand, the bandwidth at the WiMAX frequency 5.8 GHz is much wider as this frequency can

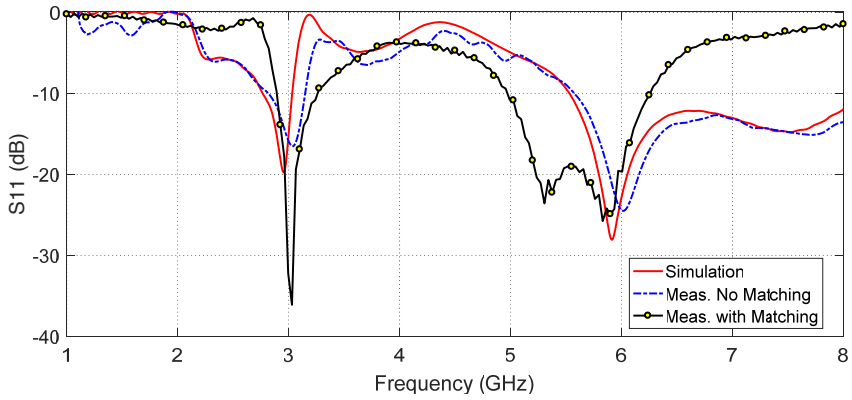

Figure 11. Comparison between the measured frequency response of the reflection coefficient $|S_{11}|$ of the proposed conical-helix/monopole antenna and that obtained by electromagnetic simulation using the commercially available CST® simulation package.

be considered a travelling-wave antenna, which enables the central on-body antenna to transmit data at much higher speed and, thus, facilitates the transmission of large data records of the patient state through the WiMAX communication system.

As shown in the figure, the attachment of the matching elements to the wire antenna, as presented in Figure 8(b), leads to improving the impedance matching such that wider bandwidths are obtained for VSWR < 1.5 (i.e., $|S_{11}| \leq -15$ dB) around the two operational frequencies. A VSWR lower than 1.5 is an important requirement for the target application (to save the power of the return loss) so as to get a low-power WBAN antenna.

6.2. Simulation and Experimental Assessment of the Radiation Patterns of the Proposed On-Body Antenna

The CST® simulation package is used to evaluate the far-field radiation patterns produced by the conical-helix/monopole antennas at 3.0 GHz and 5.8 GHz using the three-layer model of the human body described in Section 3.

On the other hand, the experimental setups for measuring the radiation patterns of the proposed antenna using the VNA of the Agilent Field Fox N9918A while being placed in free space and mounted on the human body are shown in Figures 12 and 13, respectively. A reference right-hand circularly polarized helical antenna is connected to port '2' of the VNA whereas the antenna under test is connected to port '1' to obtain its radiation pattern by measuring the transmission coefficient $|S_{21}|$ at the frequencies of concern.

The dependence of the maximum gain of the proposed conical-helix/monopole antenna when being placed on the human body is presented in Figure 14. The measured gain shows good agreement with that obtained using electromagnetic simulation. The measured gain at 3.0 GHz is about 2.3 dBi, which is very close to that of a monopole on ground plane. The antenna has a higher gain (about 8 dBi) at 5.8 GHz, which shows end fire radiation from the conical helix antenna.

6.2.1. Radiation Patterns at 30 GHz

The radiation pattern produced by the conical-helix/monopole antenna at 3.0 GHz is obtained by electromagnetic simulation when the antenna is placed in free space. Also, the experimental setup shown in Figure 12 is used to measure the radiation pattern at the same frequency. The two-dimensional radiation patterns obtained by simulation and experimental measurements are presented in Figure 15 in comparison to each other showing good agreement. As shown in this figure, the radiation pattern is omnidirectional in the azimuth plane and broadside in the elevation planes with null in the direction parallel to the antenna axis (i.e., normal to the human body surface). The quarter-wavelength monopole

Figure 12. Experimental setup for measuring the radiation pattern of the proposed on-body conical-helix monopole antenna in free space using the VNA of the Agilent Field Fox N9918A.

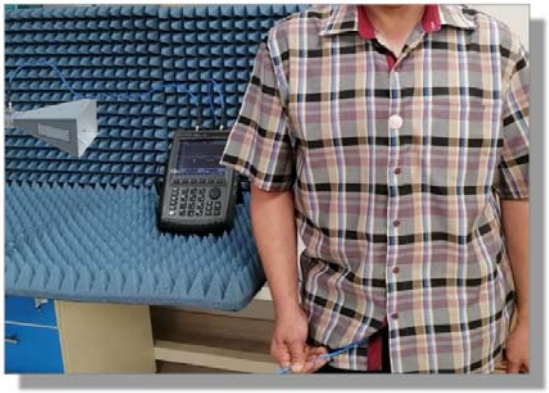

Figure 13. Experimental setup for measuring the radiation patterns of the conical-helix/monopole antenna when mounted on the human body using the VNA of the Agilent Field Fox N9918A.

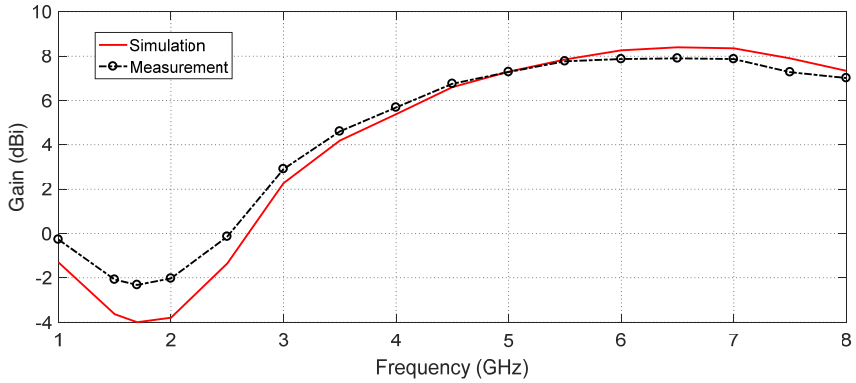

Figure 14. Frequency response of the maximum gain of the proposed conical-helix/monopole antenna (placed on the human body); the antenna dimensions are $H_M = 18.5\,\text{mm}$, $H_H = 18.5\,\text{mm}$, $\theta_H = 28^\circ$, $D_H = 20\,\text{mm}$.

produces a linear polarized electric fields, and the shape of the radiation pattern means that the monopole is an active part of the composite wire antenna as it is resonant at this frequency, and consequently, it is responsible for the radiation at 3.0 GHz.

The far-field pattern produced at 3.0 GHz by the on-body antenna when it is mounted on the three-layer model of the human body described in Section 3 is obtained by electromagnetic simulation. The resulting three-dimensional radiation pattern of the total radiated field is presented in Figure 16. The experimental setup described in Figure 13 is used to evaluate the two-dimensional radiation patterns in the elevation planes when the antenna is mounted on a real human body. These patterns are presented in Figure 17 in comparison with the patterns obtained by electromagnetic simulation. As shown in the figure, the experimental measurements and simulation results show good agreement. It is clear that the radiation at this frequency is mainly produced by the monopole part of the composite structure of the wire antenna. As shown in this figure, the radiation pattern is omnidirectional in the azimuth plane and broadside in the elevation planes with null in the direction parallel to the antenna axis (normal to the body surface). Thus, the radiated power at 3.0 GHz is more directed towards the body surface or into the human tissues near the body surface than the radiation at 5.8 GHz. Such a radiation pattern makes the conical-helix/monopole antenna appropriate to perform on-body and in-body communications with the biosensor antennas. When this pattern is compared to that obtained when the antenna is placed in free space, Figure 15, it is shown that the human body has the effect of reducing the backscatter and, thus, increasing the front-to-back ratio of the radiation.

6.2.2. Radiation Patterns at 5.8 GHz

The radiation patterns produced by the conical-helix/monopole antenna at 5.8 GHz are obtained by electromagnetic simulation when the antenna is placed in free space. Also, the experimental setup shown in Figure 12 is used to measure the corresponding radiation patterns at the same frequency. The two-dimensional radiation patterns of the total radiated electric field obtained by electromagnetic simulation and experimental measurements are presented in Figures 18(a) and 18(b) at the two planes, $\phi = 0, 180°$, and $\phi = 90, 270°$, respectively, in comparison to each other showing good agreement. As shown in this figure, the radiation patterns show omnidirectional radiation in the azimuth plane and end-fire (balloon-like) radiation in the elevation planes. The maximum radiation is obtained in the direction parallel to the antenna axis. This shape of the radiation pattern means that conical helix is an active part of the composite wire antenna at this frequency, and consequently, it is responsible for the radiation at 5.8 GHz. As the conical helix produces left-hand circular polarized electric fields, the left and right-hand radiation patterns are plotted in Figures 18(c) and 18(d) at the two planes, $\phi = 0, 180°$,

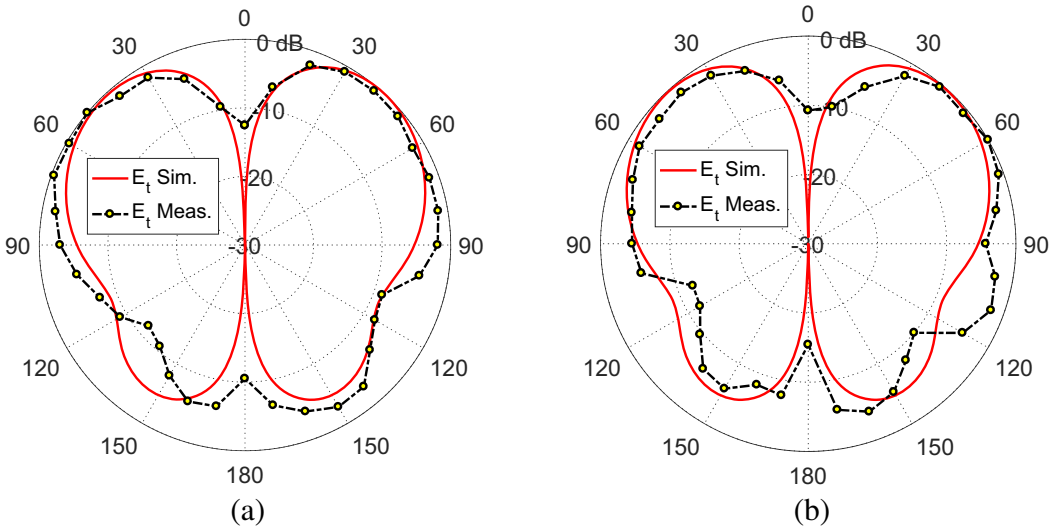

Figure 15. Comparison between the radiation patterns obtained by simulation and experimental measurements for the total field produced by the conical-helix/monopole antenna (placed in free space) in the planes, (a) $\phi = 0, 180°$, and (b) $\phi = 90, 270°$, $f = 3.0$ GHz; the antenna dimensions are $H_M = 18.5$ mm, $H_H = 18.5$ mm, $\theta_H = 28°$, $D_H = 20$ mm, $f = 3$ GHz.

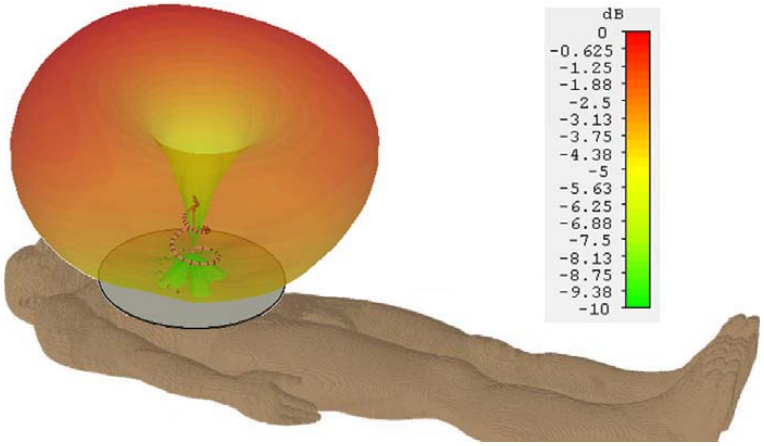

Figure 16. Three-dimensional far-field radiation pattern of the on-body conical-helix/monopole antenna of dimensions, $H_M = 18.5$ mm, $H_H = 18.5$ mm, $\theta_H = 28°$, $D_H = 20$ mm, $f = 3.0$ GHz.

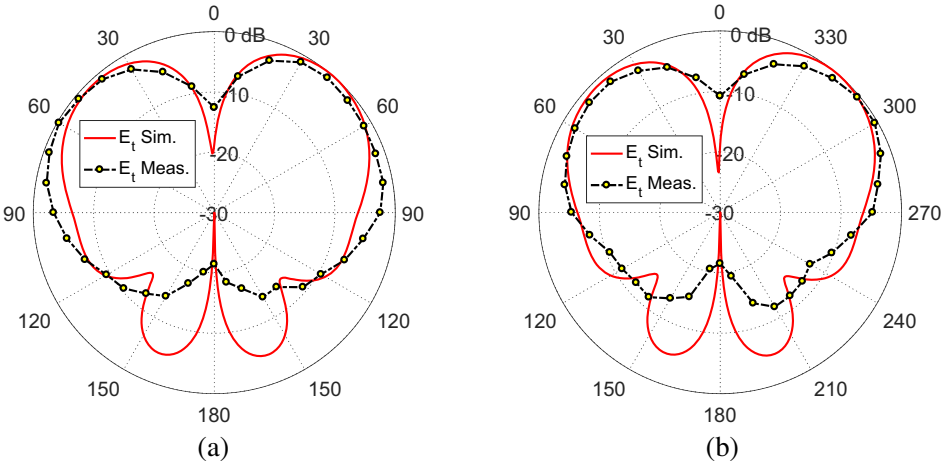

Figure 17. Comparison between the patterns obtained by simulation and experimental measurements for the total field produced by the conical-helix/monopole antenna (placed on the human body) in the planes, (a) $\phi = 0,\ 180°$, and (b) $\phi = 90,\ 270°$, $f = 3.0\,\text{GHz}$; the antenna dimensions are $H_M = 18.5\,\text{mm}$, $H_H = 18.5\,\text{mm}$, $\theta_H = 28°$, $D_H = 20\,\text{mm}$.

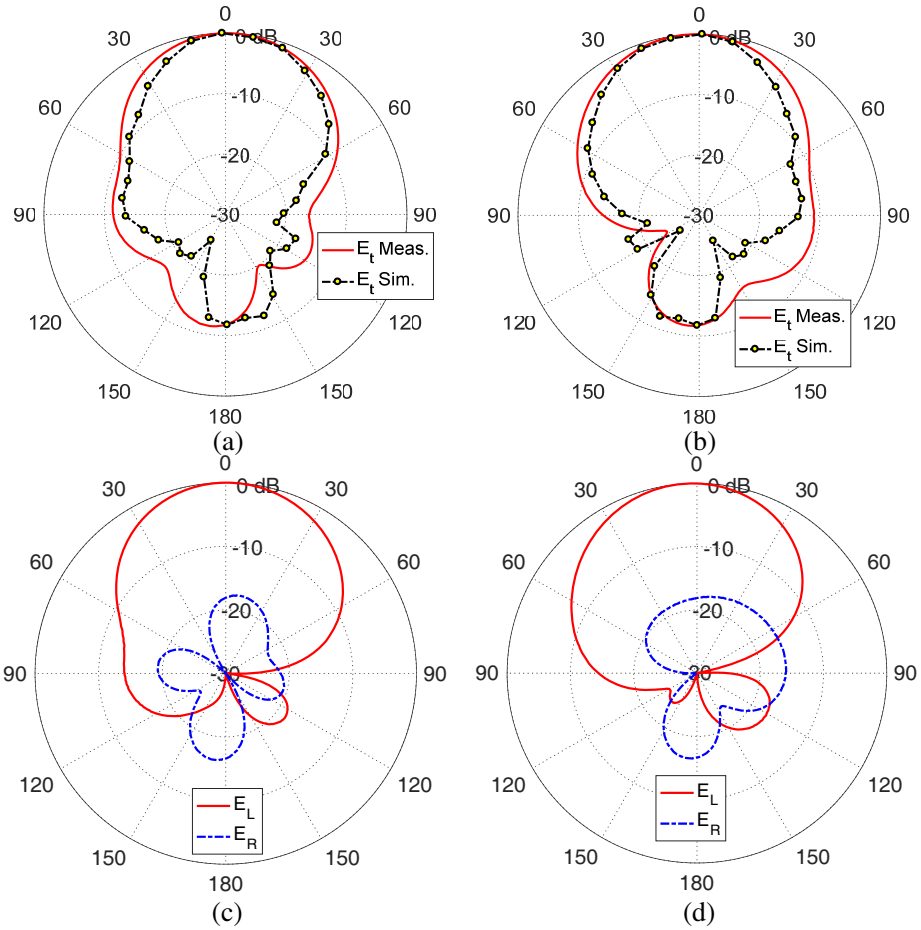

Figure 18. Comparison between the simulated and measured far-field radiation patterns for the conical helix antenna of the total electric field in the planes (a) $\phi = 0,\ 180°$, and (b) $\phi = 90,\ 270°$, and of the right-hand and left-hand circular polarization in the planes, (c) $\phi = 0,\ 180°$, and (d) $\phi = 90,\ 270°$, $f = 5.8\,\text{GHz}$; the antenna dimensions are $N_T = 3$, $H_M = 18.5\,\text{mm}$, $H_H = 18.5\,\text{mm}$, $\theta_H = 28°$, $D_H = 20\,\text{mm}$.

and $\phi = 90, 270°$, respectively.

The far-field pattern produced at 5.8 GHz by the proposed on-body antenna when it is mounted on the three-layer model of the human body as described in Section 3 is obtained by electromagnetic simulation. The three-dimensional radiation pattern of the total radiated field is presented in Figure 19. The experimental setup described in Figure 13 is used to evaluate the two-dimensional radiation patterns in the elevation planes when the antenna is mounted on a real human body. These patterns are presented in Figure 20 in comparison with the patterns obtained by electromagnetic simulation. As shown in the

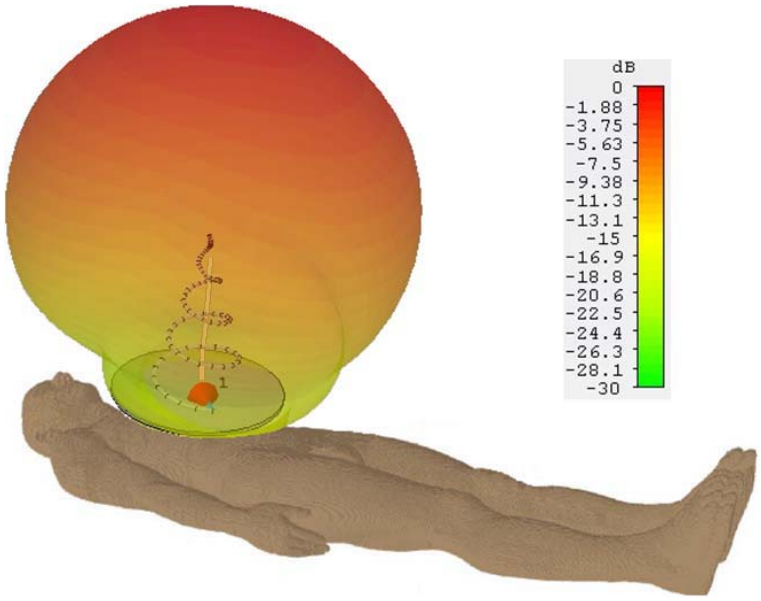

Figure 19. Three-dimensional radiation pattern of total field produced by the on-body conical-helix/monopole antenna of dimensions, $N_T = 3$, $H_M = 18.5\,\text{mm}$, $H_H = 20\,\text{mm}$, $\theta_H = 28°$, $D_H = 20\,\text{mm}$, $f = 5.8\,\text{GHz}$.

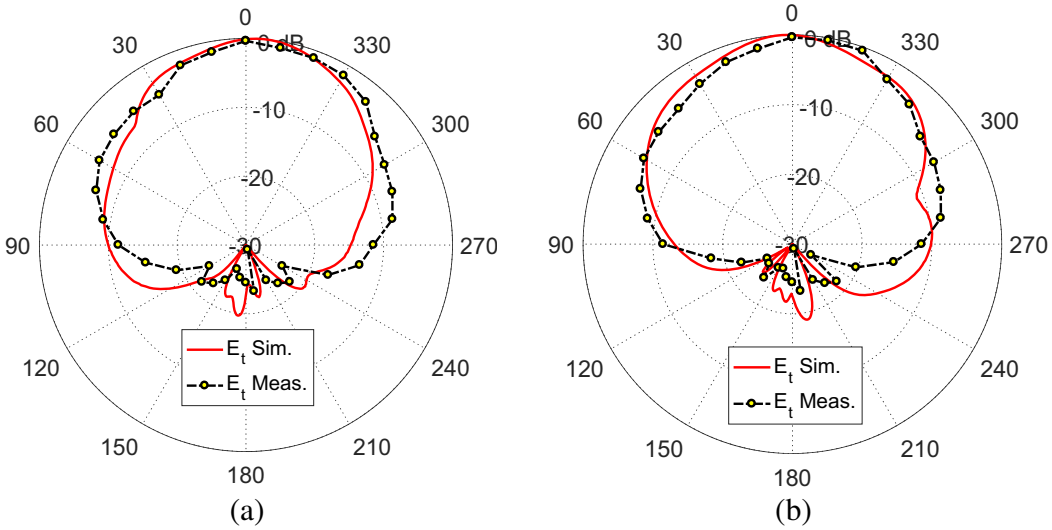

Figure 20. Comparison between the patterns obtained by simulation and experimental measurements for the total field produced by the conical-helix/monopole antenna (placed on the human body) in the planes, (a) $\phi = 0, 180°$, and (b) $\phi = 90, 270°$, $f = 5.8\,\text{GHz}$; the antenna dimensions are $N_T = 3$, $H_M = 18.5\,\text{mm}$, $H_H = 18.5\,\text{mm}$, $\theta_H = 28°$, $D_H = 20\,\text{mm}$.

figure, the experimental measurements and simulation results show good agreement. It is clear that the radiation at this frequency is mainly produced by the conical helix part of the composite structure of the wire antenna. As shown in this figure, the radiation pattern is omnidirectional in the azimuth plane and end-fire (balloon-like) in the elevation planes with maximum in the direction parallel to the antenna axis. Thus, the radiated power at 5.8 GHz is mainly directed towards the WiMAX antenna mounted in the room ceil, which is appropriate for off-body communications intended at this frequency. Moreover, such a radiation pattern is appropriate to keep the main radiation at this frequency far from the human body to reduce the SAR in the human tissues.

6.2.3. Effect of the Diameter of the Copper Circular Disc on the Radiation Patterns

For reducing the antenna size, the diameter of the copper circular disc can be reduced from 40 mm to 20 mm. When the antenna is mounted on the human body, the radiation patterns produced at 3.0 GHz and 5.8 GHz are presented in Figures 21 and 22, respectively, for different values of the copper disc. It is shown that the radiation patterns at the two frequencies are almost independent of the copper disc size. Using the smallest copper disc of those antennas whose results are presented in the figure gives antenna dimensions of 20 mm × 18.5 mm as that shown in Figure 1(a). Such a small antenna can be used as a button-like wearable antenna attached to the clothes of the patient as shown in Figures 1(a) and 1(b).

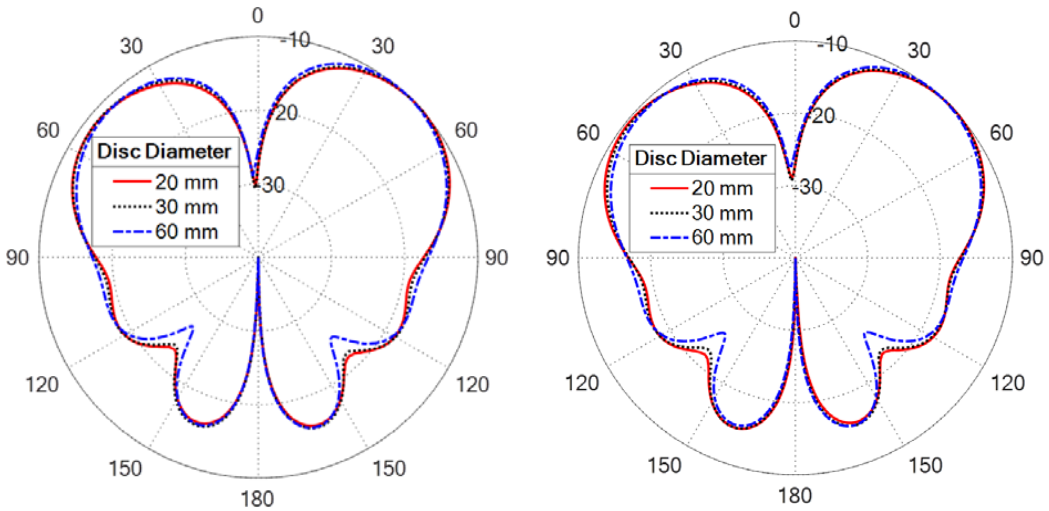

Figure 21. Comparison between the patterns obtained by simulation for the total field produced by the conical-helix/monopole antenna (placed on the human body) in the planes (a) $\phi = 0, 180°$, and (b) $\phi = 90, 270°$, for different values of the copper circular disc diameter, $f = 3.0$ GHz; the antenna dimensions are $N_T = 3$, $H_M = 18.5$ mm, $H_H = 18.5$ mm, $\theta_H = 28°$, $D_H = 20$ mm.

6.3. Power Density and SAR Distribution in the Human Tissues due to Radiation from the Proposed On-Body Antenna

This section is concerned with the experimental measurement and numerical assessment of the power density distribution on the surface of the human body at 3.0 GHz when the proposed conical-helix/monopole antenna is mounted on the human body as shown in Figures 2 and 13. Also, the numerical results concerned with the SAR distribution in the different tissues of the three-layer human body model described in Section 3 are presented and discussed.

For experimental assessment of the power density distribution on the human body surface, the radiation hazard meter Extech® model 480846 is used with its isotropic probe touching the human body as shown in Figure 23 while the conical-helix/monopole antenna (covered with the radom) is

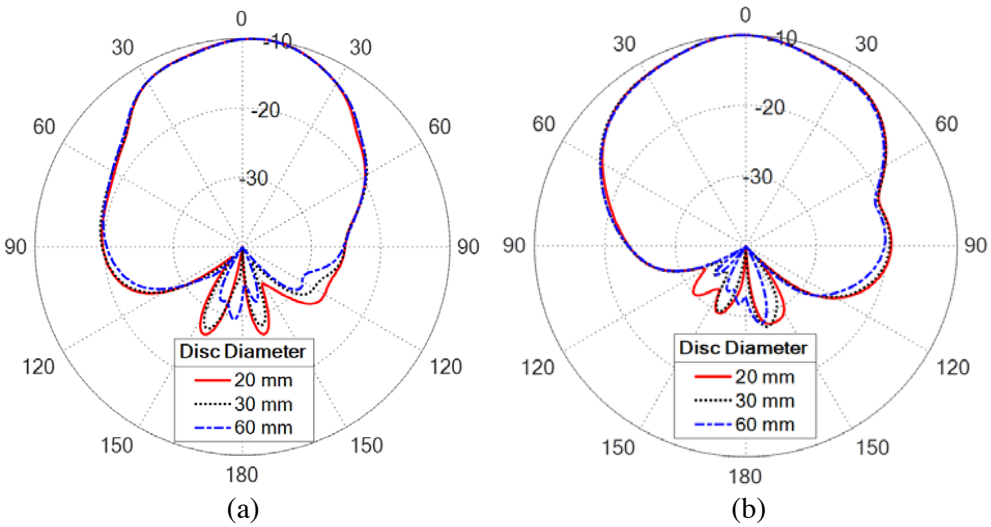

Figure 22. Comparison between the patterns obtained by simulation for the total field produced by the conical-helix/monopole antenna (placed on the human body) in the planes (a) $\phi = 0, 180°$, and (b) $\phi = 90, 270°$, for different values of the copper circular disc diameter, $f = 5.8\,\text{GHz}$; the antenna dimensions are $N_T = 3$, $H_M = 18.5\,\text{mm}$, $H_H = 18.5\,\text{mm}$, $\theta_H = 28°$, $D_H = 20\,\text{mm}$.

Figure 23. Measurement of the power density distribution near the skin of the body using the radiation hazard meter Extech® model 480846 when the conical helix antenna is excited with input power $P_{in} = 0\,\text{dBm}$ at $f = 3.0\,\text{GHz}$, (a) The antenna is oriented with tip pointing to the power density meter. (b) The antenna is oriented with tip pointing to the room ceil (normal operation); the antenna dimensions are $N_T = 3$, $H_M = 18.5\,\text{mm}$, $H_H = 18.5\,\text{mm}$, $\theta_H = 28°$, $D_H = 20\,\text{mm}$, $f = 3\,\text{GHz}$.

placed on the patient chest and excited with input power $P_{in} = 0\,\text{dBm}$ (1 mW) at $f = 3.0\,\text{GHz}$. The power density meter shows a reading of $0.041\,\mu\text{W/cm}^2$ when the antenna is oriented with its tip pointing to the power density meter as shown in Figure 23(a). When the antenna is oriented with the tip of the conical helix pointing to the room ceil (normal operation), the reading of the power density meter is $0.276\,\mu\text{W/cm}^2$ as shown in Figure 23(b). The comparison of the two readings of the power density meter, taking the orientations of the antenna into consideration, indicates that the radiation of the conical helix antenna has mainly broadside radiation at this frequency. However, the maximum level of

the power density still ensures safe values of the electromagnetic exposure.

Figure 24(a) presents the distribution of the microwave power density just on the skin surface over the rectangular area surrounded by the blue dashed rectangle shown in Figure 6 due to the placement of the conical-helix/monopole antenna with its base touching the human body surface while the antenna is excited by input power $P_{in} = 0\,\text{dBm}$ at $f = 3.0\,\text{GHz}$. It is shown that the maximum power density on the skin does not exceed $0.035\,\text{mW/cm}^2$, which ensures the safe level of electromagnetic exposure. The corresponding SAR distributions in the tissues of skin, fat, and muscle over the area of interest are presented in Figures 24(b), 24(c), and 24(d). It is shown that the maximum value of the SAR occurs in the skin tissues whereas the fat tissues have the minimum value of the SAR due to the higher conductivity of the skin tissue and larger depth of the fat tissues inside the human body. It is shown

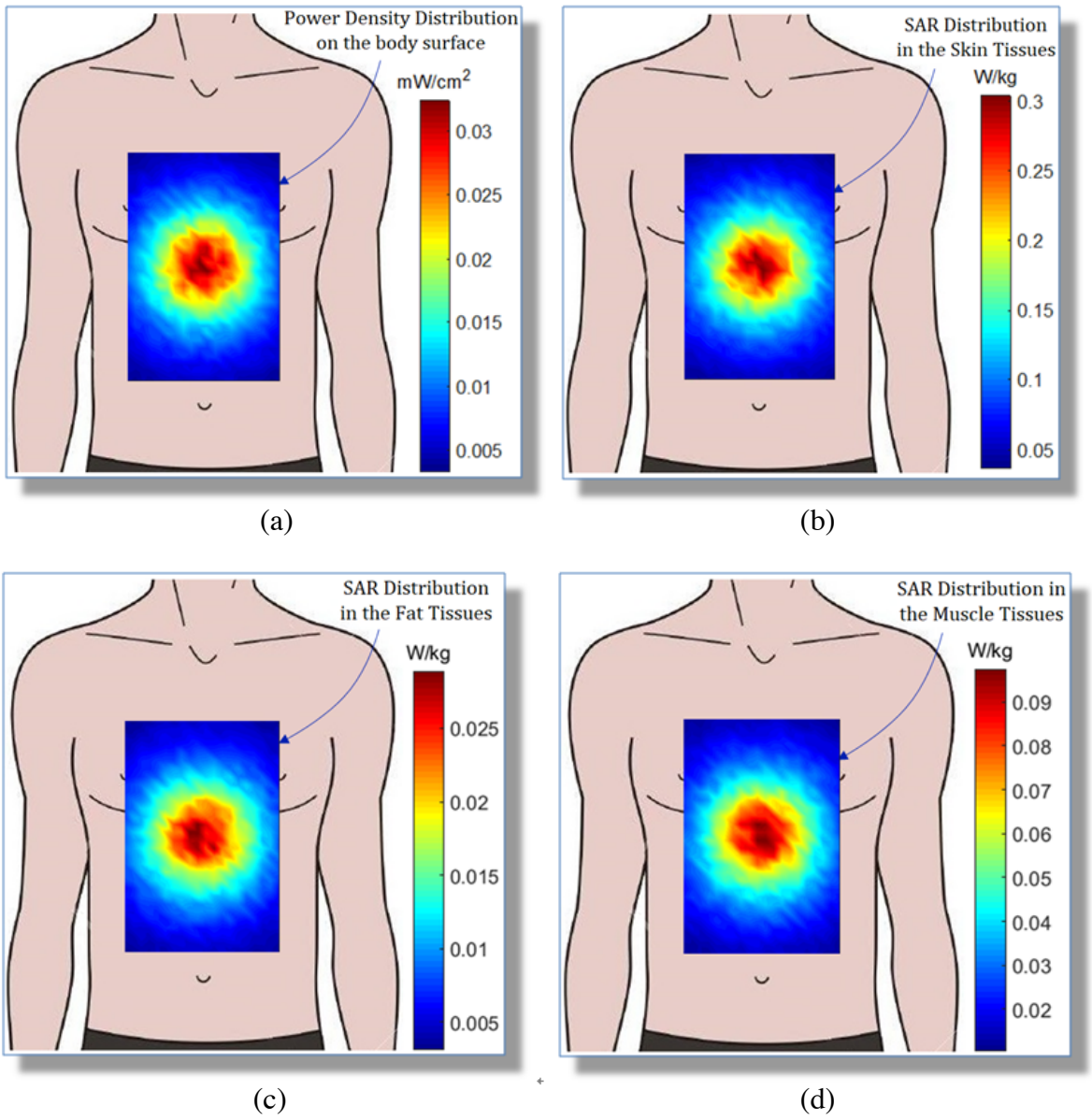

Figure 24. Distribution of (a) microwave power density on the surface of the body, (b) SAR in the skin tissues, (c) SAR in the fat tissues, and (d) SAR in muscle tissues, due to conical-helix/monopole antenna fed with input power $P_{in} = 0\,\text{dBm}$ at $f = 3.0\,\text{GHz}$; the antenna dimensions are $N_T = 3$, $H_M = 18.5\,\text{mm}$, $H_H = 18.5\,\text{mm}$, $\theta_H = 28°$, $D_H = 20\,\text{mm}$.

that the maximum SAR in all the tissue types does not exceed 0.3 W/kg, which ensures the safe level of electromagnetic exposure.

6.4. Assessment of the WBAN Communication System Performance Using the Proposed On-Body Antenna

This section is concerned with the presentation of some numerical results for the assessment of the performance of the WBAN communication system described in Section 2 according to the channel model described in Section 5. It is assumed that all the biosensor antennas (both on-body and in-body) in the WBAN are isotropic and lossless and distributed on the surface of the human body. The losses are caused only by the microwave propagation inside the lossy tissues on the surface of the human body.

6.4.1. Distribution of the SNR and BER on the Skin due to the Proposed On-Body Antenna

The distribution of the SNR due to AGWN of power spectral density $N_0/2 = 1 \times 10^{-3}$ mW/Hz at isotropic receiving biosensor antennas distributed on the skin surface over the rectangular area (indicated by the dashed rectangle in Figure 6 is presented in Figure 25(a) using the shown color code when the operating frequency is 3.0 GHz, and the input power to the conical-helix/monopole antenna is 0 dBm (1 mW). The corresponding distributions of BER over the same area of the human body surface are presented in Figures 25(b) and 25(c) under the assumption of using 8-symbol and 16-symbol in the M-ary PSK modulation technique, respectively. In spite of the low power fed to the proposed on-body conical-helix/monopole antenna (only 1 mW) and thanks to the optimized design of this antenna, the BER does not exceed 1.2×10^{-6} and 5.3×10^{-4} for the two modulation schemes.

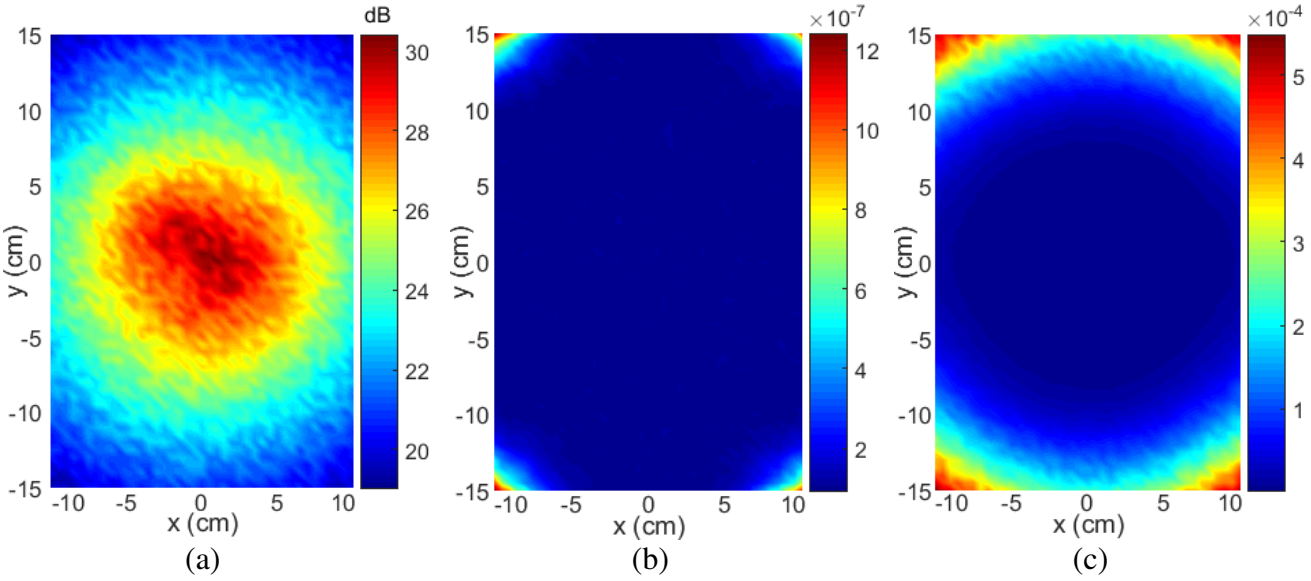

Figure 25. Distribution of the SNR and the corresponding BER over the area of the skin within which the (isotropic) biosensor antennas are allocated due to a central on-body conical-helix/monopole antenna fed with input power, $P_{in} = 0$ dBm at $f = 3.0$ GHz, (a) SNR, (b) BER for 8-symbol PSK, (c) BER for 16-symbol PSK, the antenna dimensions are $N_T = 3$, $H_M = 18.5$ mm, $H_H = 18.5$ mm, $\theta_H = 28°$, $D_H = 20$ mm, $f = 3.0$ GHz.

6.4.2. Dependence of the SNR and BER on the Height of the On-Body Antenna above the Skin

The height at which the conical-helix/monopole antenna (proposed for on-body communications in WBANs) is placed has a significant effect on the SNR and BER as shown in Figures 26(a) and 26(b), respectively, for different values of the input power to the proposed on-body conical-helix/monopole

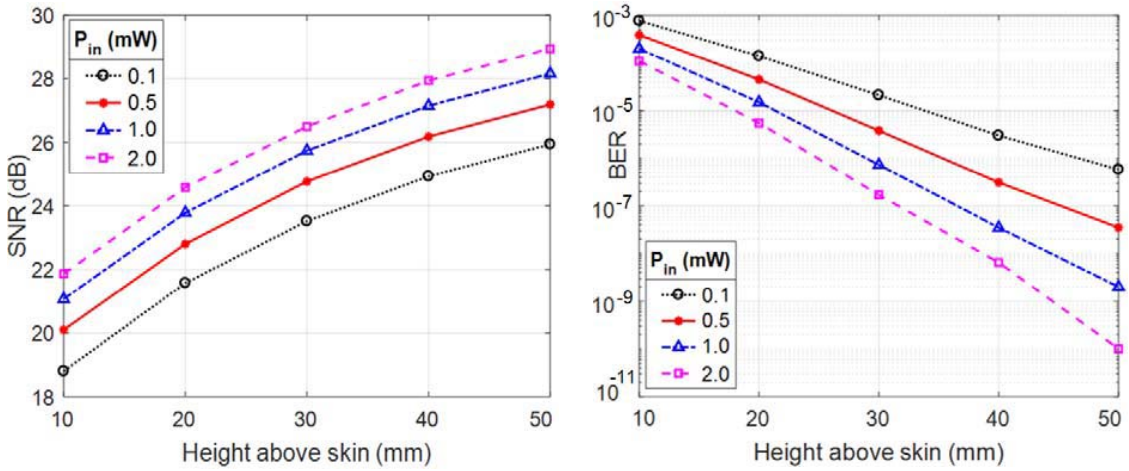

Figure 26. Dependence of the minimum SNR and the corresponding BER on the height at which the conical-helix/monopole antenna is placed above the surface of the human body when used in WBAN as a central on-body antenna fed with different values of the input power at $f = 3.0\,\text{GHz}$, (a) minimum SNR, (b) maximum BER.

antenna. As shown in these figures, the SNR is increased, and hence, the BER is decreased with increasing the height of the conical helix above the surface of the human body. Thus, it is preferable to place the antenna at a higher level above the surface of the human body for better performance of the communication system (i.e., higher SNR and lower BER).

Definitely, it is clear that the BER is decreased as the antenna is placed as far as possible from the human body surface. However, even when the antenna is placed at a height of 1 cm a BER of less than 10^{-4} is still achievable, which can be fairly acceptable.

7. CONCLUSION

A dual-band conical-helix/monopole antenna is proposed to operate as a central on-body antenna for WBAN. The characteristics of this antenna are investigated through electromagnetic simulation and experimental measurements. The antenna is designed to produce end-fire (balloon-like) radiation to communicate (through its far-field) with the WiMAX antenna at 5.8 GHz and to produce broad-side (figure of eight) radiation to communicate (through its near or far field) with the on-skin biosensor antennas at 3.0 GHz. A prototype of the proposed antenna is fabricated for experimental assessment. The antenna is matched with $50\,\Omega$ coaxial feeder over the operational frequency bands, mounted on a copper circular disc, and covered with a very thin dielectric radom for mechanical protection. The radiation patterns obtained by experimental measurements show good agreement with those obtained by electromagnetic simulation and are shown to be appropriate for communication with the WiMAX antenna and the biosensor antennas at 5.8 GHz and 3.0 GHz, respectively. The SAR distributions inside the human tissues of concern (skin, fat and muscle) are evaluated showing a safe level of electromagnetic exposure. Quantitative assessment of the WBAN communication system performance is achieved when the proposed antenna is employed as on-body central antenna for the WBAN. Owing to the optimized design of the proposed antenna, the BER is shown to have very low BER even when the input power fed to the antenna is only 1 mW.

REFERENCES

1. Jeerapan, I. and S. Poorahong, "Review — Flexible and stretchable electrochemical sensing systems: Materials, energy sources, and integrations," *J. Electrochem. Soc.*, Vol. 167, 037573, 2020.

2. Mahfouz, M. R., M. J. Kuhn, G. To, and A. E. Fathy, "Integration of UWB and wireless pressure mapping in surgical navigation," *IEEE Transactions on Microwave Theory and Techniques*, Vol. 57, No. 10, 2550–2564, 2009.
3. Vallejo, M., J. Recas, P. G. del Valle, and J. L. Ayala, "Accurate human tissue characterization for energy-efficient wireless on-body communications," *Sensors*, Vol. 13, No. 6, 7546–7569, 2013.
4. Gemio, J., J. Parron, and J. Soler, "Human body effects on implantable antennas for ISM bands applications: Models comparison and propagation losses study," *Progress In Electromagnetics Research*, Vol. 110, 437–452, 2010.
5. Grimm, M., D. Manteuffel, R. Thomä, R. H. Knöchel, J. Sachs, I. Willms, and T. Zwick, "Antennas and propagation for on-, off- and in-body communications," *Ultra-Wideband Radio Technologies for Communications, Localization and Sensor Applications*, InTech., 2013.
6. Kang, S. and C. W. Jung, "Wearable fabric reconfigurable beam-steering antenna for on/off-body communication system," *International Journal of Antennas and Propagation*, ID 539843, Hindawi Publishing Corporation, 2015.
7. Islam, M. N. and M. R. Yuce, "Review of medical implant communication system (MICS) band and network," *Science Direct, ICT Express*, Vol. 2, 188–194, 2016.